

Model plasma membrane indicates the inner leaflet  
is poised to initiate compositional heterogeneities

H. Giang and M. Schick

August 23, 2016

## Abstract

We investigate a model of an asymmetric bilayer consisting of sphingomyelin, phosphatidylcholine, and cholesterol in the outer leaflet, and phosphatidylethanolamine, (PE), phosphatidylserine, and cholesterol in the inner leaflet. Composition fluctuations are coupled to membrane fluctuations via the bending energy which depends upon the local spontaneous curvature dominated by the PE in the inner leaflet. This brings about a microemulsion in that leaflet with a characteristic wavelength of 37 nm as shown by the PE-PE structure function. Thus the inner leaflet will respond to an external perturbation most strongly at this length. However the correlation length is approximately 1 nm so that composition variations are not seen in the inner leaflet itself. Depending upon the strength of the coupling between leaflets, the outer leaflet is either a normal fluid or is also a microemulsion. In this model then, the lipids of the plasma membrane would not evince inhomogeneities, but would be primed to create them from the inner leaflet in response to non-lipid perturbations.

# 1 Introduction

The hypothesis that the distribution of lipids of the plasma membrane is not homogeneous, but rather is characterized by inhomogeneities, denoted “rafts”, that can serve as platforms for protein function continues to draw much attention. However much of the evidence for such inhomogeneities is indirect (1). Furthermore there is no agreement on a physical mechanism that would bring about such inhomogeneities, although several have been proposed. If proteins attract some lipids in preference to others, then the aggregation of proteins would be reflected in an inhomogeneous distribution of lipids. Other mechanisms which do not require the presence of proteins have also been proposed. For example, an excess of lipids in one region could result from liquid-liquid phase separation (2). Indeed *in vitro* ternary mixtures of a saturated lipid, representing sphingomyelin (SM) in the plasma membrane, an unsaturated lipid, like phosphatidylcholine (PC), and cholesterol do undergo such a phase transition at biologically relevant temperatures (3). Large macroscopically phase-separated regions have, in fact, been observed in yeast vacuoles (4), but never in plasma membranes. This may be due to the fact that the inner leaflet of the plasma membrane consists almost entirely of unsaturated lipid so that there is little tendency for phase separation of unsaturated and saturated lipids (5). It could then be argued that in the plasma membrane the critical temperature for phase separation is below biological temperatures, and that the inhomogeneities are due to fluctuations of a nearby critical point (6). If so, one has to understand why so many different systems are just poised at the necessary distance from a critical point that the fluctuations are just of the size thought to characterize rafts, between 10 and 100 nm. Further, as noted above, there is little tendency for the inner leaflet to undergo phase separation at all. A third line of thought is that the inhomogeneities indicate that the lipid membrane is a two-dimensional microemulsion, a fluid with dynamic but well-defined structure. Three-dimensional microemulsions, often consisting of oil, water, and an amphiphile are, of course, very well-known (7). The question then arises as to what molecule plays the role of an amphiphile in the plasma membrane. Safran and co-workers (8, 9) have argued that the unsaturated lipids can play such a role by orienting themselves at, or near, the interface between saturated lipid-rich and saturated lipid-poor regions. There is experimental evidence, however, that this mechanism is not the origin of compositional inhomogeneities (10). That microemulsions could, nonetheless, be the source of compositional variations was noted by one of us (11) observing that microemulsions can be produced by mechanisms that do not

require an amphiphile. Any mechanism that can produce modulated phases can produce a microemulsion as the latter can be thought of as resulting from the melting, or disordering, of the former. Modulated phases have indeed been observed in mixtures of three, or four lipids (12–14) and in yeast vacuoles (4) which renders plausible the idea that the plasma membrane might be characterized as a microemulsion.

Two mechanisms that could bring about modulated phases and microemulsions without an amphiphile have been proposed. Recently Amazon et al. (15) noted that a membrane bending modulus which varied with the local composition could bring about modulated phases on a closed bilayer vesicle. Earlier, Schick (11) noted that there was a significant difference between the large spontaneous curvature of PE and the relatively small one of PS, and therefore proposed that the coupling of membrane fluctuations and a compositionally-dependent spontaneous curvature (16) could be the mechanism at work. Just such a cholesterol-dependent spontaneous curvature of PE was recently invoked by us (17) to explain the several observations that cholesterol is located preferentially in the cytoplasmic leaflet of the plasma membrane (18–21). It is this mechanism that we shall invoke in this paper.

Because this significant difference in spontaneous curvature of the components is only characteristic of the cytoplasmic layer, we must treat an asymmetric bilayer, as had been done earlier by Shlomovitz and Schick (22). In that paper, however, the role of cholesterol was ignored, and the system was characterized by one order parameter in each leaflet. In this paper, we include cholesterol explicitly and characterize each leaflet by three components; SM, PC, and cholesterol in the outer leaflet, PE, PS, and cholesterol in the inner leaflet. Furthermore we require that the chemical potentials of the cholesterol in each leaflet be equal reflecting the rapid exchange of cholesterol between leaflets (23, 24). Our model is reviewed in the next section. We calculate structure functions between various components, in particular the PE-PE and SM-SM structure functions. We find that over a wide range of compositions of the inner leaflet, the PE-PE structure functions have a maximum at a non-zero wave number, a feature characteristic of a microemulsion. The wave number corresponds to a length of about 37 nm. The behavior of the structure function indicates that the inner leaflet evinces the largest response at this distance from a perturbation. The SM-SM structure function shows that the outer leaflet is either a normal fluid or a microemulsion depending upon the strength of the coupling between the two leaflets. We also examine the two-particle PE-PE correlation function of the inner leaflet obtained from the structure function. It has the form of an exponentially damped oscillatory function. However the correlation length,

which sets the scale of the exponential damping, is in general considerably smaller than the wavelength of the oscillations. As a consequence, the only observable remnant of the oscillations is that the correlation function decays to zero from negative values. Consequently, while the system is quite susceptible to perturbations of a large size, it does not, of itself, display inhomogeneities at such a length scale.

## 2 Materials and Methods

We consider a bilayer which contains PS, PE, and cholesterol in the inner leaflet, and SM, PC, and cholesterol in the outer leaflet. Further, as we know that cholesterol tends to order the chains of the other lipids, particularly the saturated chains of SM, we consider there to be two populations of SM; those with more-ordered chains,  $SM_{or}$ , and those with less-ordered chains,  $SM_{dis}$ . These populations freely convert between one another. This description can produce (25, 26) the closed-loop phase diagram observed in some ternary mixtures (27). We denote the number of molecules of each component in the inner leaflet by  $N_{PE}$ ,  $N_{PS}$  and  $N_{C_i}$ , and the total number of molecules in the inner leaflet by  $M_I$ . Similarly denote the number of molecules of each component in the outer leaflet by  $N_{SM_{or}}$ ,  $N_{SM_{dis}}$ ,  $N_{PC}$ , and  $N_{C_o}$  and the total number of molecules in the outer leaflet by  $M_O$ . Then the mol fractions of the  $i$ 'th component is  $x_i = N_i / (M_I + M_O)$ . It is more convenient to work with the mol fractions defined in each leaflet separately rather than in the total bilayer. Thus we introduce the mol fractions of the  $j$ 'th component in the inner and outer leaflets,

$$y_j = \begin{cases} \frac{N_j}{M_I}, & \text{if } j = PS, PE, C_i, \\ \frac{N_j}{M_O}, & \text{if } j = SM_{or}, SM_{dis}, PC, C_o. \end{cases} \quad (1)$$

We consider all lipids, save cholesterol, to have the same area per lipid,  $a = 0.7 \text{ nm}^2$ , and take that of cholesterol to be  $r_a a = 0.4 \text{ nm}^2$  (28, 29). We assume that the areas of the two leaflets are equal which determines the ratio of molecules in the inner leaflet,  $N^{(i)}$ , to that in the outer leaflet,  $N^{(o)}$

$$\frac{N^{(i)}}{N^{(o)}} = \frac{1 - (1 - r_a)y_{C_o}}{1 - (1 - r_a)y_{C_i}}. \quad (2)$$

From this, we can express the mol fraction of the total amount of cholesterol in the bilayer in terms of  $y_{C_i}$  and  $y_{C_o}$ :

$$x_C = \frac{y_{C_i} + y_{C_o} - 2(1 - r_a)y_{C_i}y_{C_o}}{2 - (1 - r_a)(y_{C_i} + y_{C_o})}. \quad (3)$$

The free energy of the system consists of several parts. First there is the simple, regular-solution, free energy which can be written

$$F_{rs} = \int d^2r f_{rs} \\ = \int \frac{d^2r}{a} \left[ \frac{1}{(1 - (1 - r_a)y_{c_i})} f_1(\{y_i\}) + \frac{1}{(1 - (1 - r_a)y_{c_o})} f_2(\{y_i\}) \right],$$

where the free energies per molecule are

$$\begin{aligned} f_1[T, y_{PS}, y_{PE}, y_{C_i}] &= 6\epsilon_{PS-PE} y_{PS} y_{PE} \\ &\quad + 6\epsilon_{PS-C} y_{PS} y_{C_i} + 6\epsilon_{PE-C} y_{PE} y_{C_i} \\ &\quad + k_B T (y_{PS} \log y_{PS} + y_{PE} \log y_{PE} + y_{C_i} \log y_{C_i}), \\ f_2[T, y_{SM_{or}}, y_{SM_{dis}}, y_{PC}, y_{C_o}] &= 6\epsilon_{SM_{or}-PC} y_{SM_{or}} y_{PC} + 6\epsilon_{SM_{dis}-PC} y_{SM_{dis}} y_{PC} \\ &\quad + 6\epsilon_{SM_{or}-C} y_{SM_{or}} y_{C_o} + 6\epsilon_{SM_{dis}-C} y_{SM_{dis}} y_{C_o} \\ &\quad + 6\epsilon_{PC-C} y_{PC} y_{C_o} \\ &\quad + k_B T (y_{SM_{or}} \log y_{SM_{or}} + y_{SM_{dis}} \log y_{SM_{dis}} \\ &\quad + y_{PC} \log y_{PC} + y_{C_o} \log y_{C_o}). \end{aligned} \quad (4)$$

To this we add the free energy associated with the deformation of the membrane which is described by deviations,  $h$ , from a flat configuration. There is the surface free energy

$$F_s = \int \frac{\sigma}{2} (\nabla h)^2 d^2r, \quad (5)$$

where  $\sigma$  is the surface tension, and the bending energy

$$F_b = \int \frac{\kappa}{2} (\nabla^2 h - H_0)^2 d^2r, \quad (6)$$

where  $\kappa$  is the bending modulus and  $H_0$  is the spontaneous curvature. As in our previous paper (17), we take the latter to be due solely to the PE and to depend upon the cholesterol concentration in the inner leaflet

$$H_0 = y_{PE} \left[ H_{PE} - B \frac{y_{C_i}}{y_{min}} + \frac{B}{\lambda} \left( \frac{y_{C_i}}{y_{min}} \right)^\lambda \right], \quad (7)$$

with  $B = 0.05$ ,  $y_{min} = 0.3$  and  $\lambda = 8$ . Note that the cross term in Eq. (6) couples the height fluctuations to the composition-dependent spontaneous curvature. It is this term which can bring about modulated phases and/or microemulsions.

The free energy includes the usual square-gradient term penalizing deviations from homogeneity,

$$F_p = \int \frac{1}{2} \sum_{i=1}^5 b_i |\nabla y_i|^2 d^2r. \quad (8)$$

We take  $b_i = k_B T$ . Lastly we include a direct coupling between leaflets which promotes alignment of cholesterol-rich domains

$$F_c = \int f_c d^2r = - \int \Lambda (y_{C_i} - y_{PE})(y_{C_o} - y_{PC}) d^2r. \quad (9)$$

The coupling  $\Lambda$  is not identical to the mismatch free energy defined previously (25, 30) and recently measured (31), but we expect it to be similar within an order of magnitude.

The total free energy is

$$F_{tot} = F_{rs} + F_s + F_b + F_p + F_c.$$

We utilize the two conditions

$$y_{SM_{ord}} + y_{SM_{dis}} + y_{PC} + y_{C_o} = 1, \quad (10)$$

$$y_{PE} + y_{PS} + y_{C_i} = 1 \quad (11)$$

to reduce from seven to five the number of independent mol fractions, and express the free energy in terms of them.

At equilibrium, a homogeneous phase is specified by these five mol fractions,  $y_i$ . They are determined by five conditions, as follows. From the free energy, we calculate the chemical potentials of the two classes of SM. Because the ordered and disordered SM can freely interchange, we require that their chemical potentials be equal

$$\mu_{SM_{dis}} = \mu_{SM_{or}}. \quad (12)$$

Similarly, as the cholesterol in the inner and outer leaflets can exchange freely, we require that their chemical potentials, obtained from the free energy above, be equal,

$$\mu_{C_i} = \mu_{C_o}. \quad (13)$$

The remaining three conditions are set by specifying the ratio of the total amount of SM to PC in the outer leaflet, the ratio of PS to PE in the inner leaflet, and the total mol fraction of cholesterol in the bilayer,  $x_C$ . These are known from experiment (32).

In order to determine the structure functions and correlation functions, we assume small deviations of the compositions from their equilibrium values,  $y_i$ , and small deviations  $h$  of the membrane from a flat configuration. Extensions to a closed vesicle can be carried out (33–35) but are unnecessary for our purposes. We expand the total free energy to second order in these deviations. In terms of the Fourier transforms  $h(k)$  of  $h(\mathbf{r})$  and  $y_i(k)$  of  $y_i(\mathbf{r})$  we obtain

$$\begin{aligned}
F_{tot} = & \int d^2r \left[ f_{rs}(\{y_i\}) + f_c(\{y_i\}) + \frac{\kappa}{2} H_o^2 \right] \\
& + \frac{A^2}{(2\pi)^2} \int d^2k \left[ \frac{1}{2} (\kappa k^4 + \sigma k^2) h(k) h(-k) + \kappa k^2 \mathcal{H}_0(k) h(-k) \right. \\
& \left. + \frac{1}{2} \sum_{i=1}^5 b_i k^2 y_i(k) y_i(-k) \right], \tag{14}
\end{aligned}$$

where  $\mathcal{H}_0$  is the Fourier transform of  $H_0$  when expanded to first order in the compositions; i.e.

$$\mathcal{H}_0(k) = H_0(y_{PE}, y_{c_i}) \delta_{k,0} + \frac{\partial H_0}{\partial y_{PE}} \delta y_{PE}(k) + \frac{\partial H_0}{\partial y_{c_i}} \delta y_{c_i}(k). \tag{15}$$

Upon minimizing  $F_{tot}$  with respect to  $h(k)$  we find

$$h(k) = -\frac{\kappa \mathcal{H}_0(k)}{\kappa k^2 + \sigma}, \tag{16}$$

which we substitute into  $F_{tot}$  to obtain, in Fourier space, an expression for it entirely in terms of the compositions  $y_i(k)$ . Lastly we expand this expression to second order in the  $y_i(k)$  and obtain the second variation,  $F_{tot}^{(2)}$ , in matrix form

$$\begin{aligned}
F_{tot}^{(2)} = & \frac{A^2}{(2\pi)^2} \int d^2k \{ y_{PE}(k) y_{c_i}(k) y_{SM}(k) y_{c_o}(k) \} M \{ y_{PE}(-k) y_{c_i}(-k) y_{SM}(-k) y_{c_o}(-k) \}^T \\
& \tag{17}
\end{aligned}$$

where  $y_{SM} = y_{SM_{dis}} + y_{SM_{or}}$  and  $M$  is a  $4 \times 4$  matrix. From it, the matrix of structure factors follows:  $S = M^{-1}$ . Correlation functions are obtained directly from the structure functions.

We now specify the properties of the membrane and of the interactions. We take the bending modulus to be  $\kappa = 44 k_B T$ , appropriate to



the plasma membrane (36), and the surface tension  $\sigma = 0.001k_B T/\text{nm}^2$  (37). The interactions are such that their ratios are, for the most part, taken from experiment (38), and are the same as those we have used previously (17). We have also imposed a restrictive condition that the modulated lamellar phase not be stable for any ratio of SM to PC or PS to PE. Of course the behavior of the plasma membrane for all such ratios is unknown, but we impose this condition so as to avoid prejudicing a case for the presence of a microemulsion by stabilizing a modulated phase at values of lipid ratios near those of the actual plasma membrane. This requires that we take the absolute values of the interactions to be smaller than previously corresponding to temperatures somewhat greater than those of Table 1 of Ref.(38). These interactions are, among components in the inner leaflet,  $\epsilon_{PE-C_i}/k_B T = 0.22$ ,  $\epsilon_{PS,C_i}/k_B T = -0.05$ ,  $\epsilon_{PE-PS}/k_B T = 0$ , and in the outer leaflet  $\epsilon_{PC-C_o}/k_B T = 0.16$ ,  $\epsilon_{SM_{ord}-C_o}/k_B T = -0.464$ ,  $\epsilon_{SM_{dis}-C_o}/k_B T = -0.23$ ,  $\epsilon_{SM_{ord}-PC}/k_B T = 0.24$ ,  $\epsilon_{SM_{dis}-PC}/k_B T = 0$ . For the coupling between leaflets, we take  $\Lambda = 0.01k_B T/\text{nm}^2$  (39). The ratio of the compositions of SM to PC is taken from experiment, (32)  $(x_{SM_{ord}} + x_{SM_{dis}})/x_{PC} = 1.1$ , as is that of PS to PE  $x_{PS}/x_{PE} = 0.52$ . We take the total cholesterol composition of the bilayer to be  $x_C = 0.41$  (40).

### 3 Results

We find that the components of the inner leaflet display characteristics typical of a microemulsion. In particular the structure factor  $S_{PE-PE}(k)$ , shown in Fig. 1(a), which displays the correlation between fluctuations in the concentration of PE in the inner leaflet, is characterized by a peak at a non-zero wave vector  $k = 0.17 \text{ nm}^{-1}$  which corresponds to a wavelength of  $\lambda = 37 \text{ nm}$ . The Fourier transform of this function, the PE-PE correlation function  $g(r)$ , is shown in Fig. 1(b). It displays no oscillations because the correlation length is  $\xi = 0.7 \text{ nm}$ , much shorter than the wavelength  $\lambda$ . Nonetheless, it is notable that the correlation function does not decay as a simple exponential, but approaches its asymptotic value from below, a remnant of the exponentially damped oscillatory behavior. In contrast to the inner leaflet, the outer one does not display the characteristics of a microemulsion, but rather that of a normal fluid. For example, the structure function  $S_{SM-SM}(k)$ , shown in Fig. 2(a), displays a peak at zero wave vector, and the correlation function, shown in Fig. 2(b), decays to zero from above with the same correlation length  $\xi = 0.7 \text{ nm}$ . Such a coupling of a microemulsion in one leaflet and

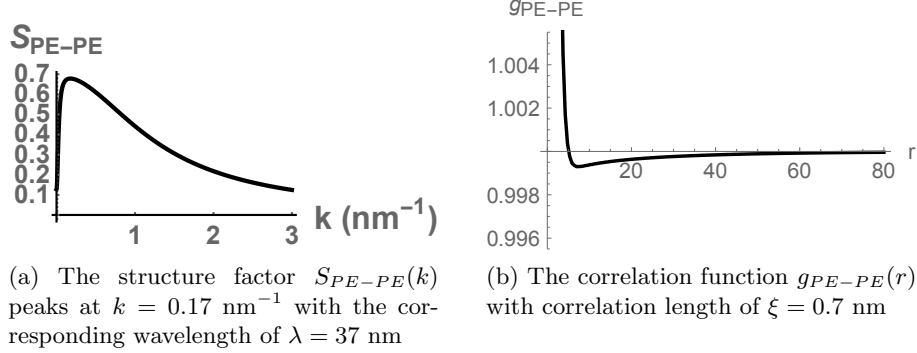


Figure 1: The correlation between fluctuations in the concentration of PE in the inner leaflet

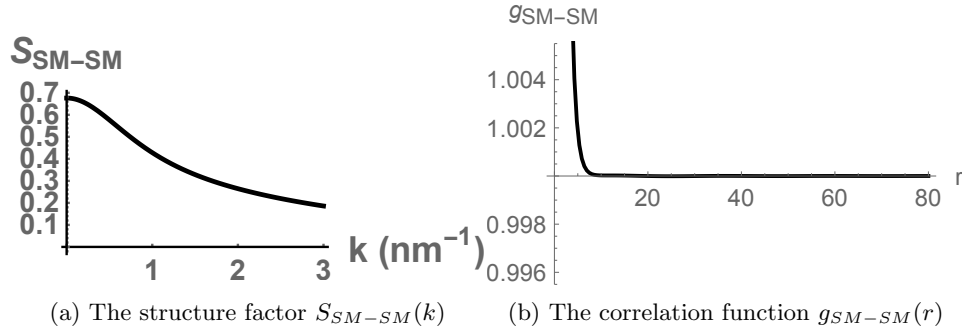


Figure 2: The correlation between fluctuations in the concentration of SM in the outer leaflet

a normal fluid in the other has been discussed previously (41, 42). If the coupling  $\Lambda$  between leaflets is increased by an order of magnitude, we find that the microemulsion in the inner leaflet is conveyed to the outer one as evidenced by the fact that  $S_{SM-SM}(k)$  now displays a peak at non-zero wave vector. The structure functions arising from fluctuations in any pair of components can be obtained. We show in Fig. 3 the  $S_{c_i-c_i}$  and  $S_{PE-c_i}$  functions. The former shows microemulsion behavior of cholesterol in the inner leaflet, and anticorrelated behavior of PE and cholesterol in the inner leaflet. Similarly Fig. 4 shows  $S_{c_o-c_o}$  and  $S_{SM-c_o}$ . These show that the outer leaflet is a normal fluid and that the SM and cholesterol in the outer leaflet are correlated as expected. Finally in Fig. 5 we display  $S_{SM-c_i}$

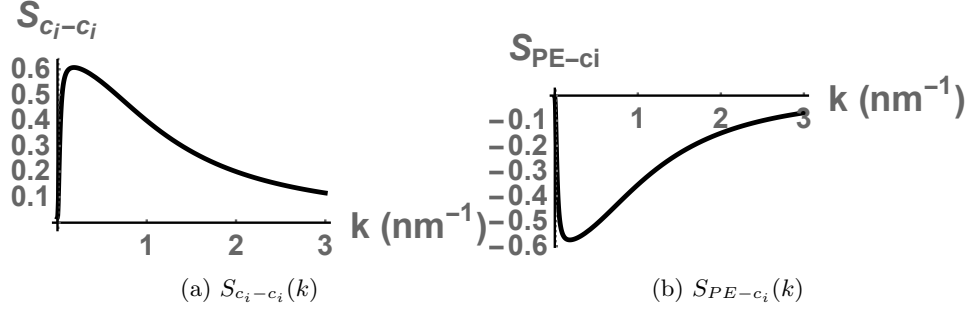


Figure 3: Two of the structure functions characterizing the inner leaflet.

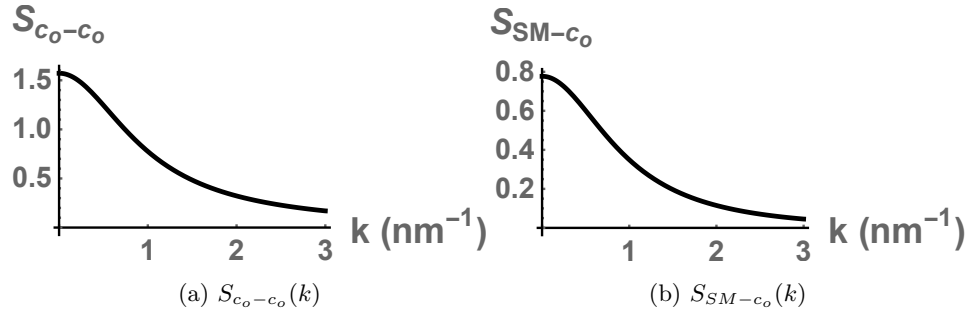


Figure 4: Two of the structure functions characterizing the outer leaflet

and  $S_{PE-c_o}$  which shows the fluctuations in SM and cholesterol in the inner leaflet to be correlated while those of PE and cholesterol in the outer leaflet to be anticorrelated. In Table 1 we show the concentrations of the various components in the two leaflets. The percentage of the total cholesterol which is in the inner leaflet is 61% in accord with most experiments which show that the cholesterol is either evenly divided between leaflets (24, 43), or more abundant in the inner leaflet (18–21, 44).

That the inner leaflet is a microemulsion is due to the coupling of the membrane curvature to the membrane spontaneous curvature, dominated by that of PE. Thus the appearance of the microemulsion in the inner leaflet depends upon the strength of this coupling. To consider this further, we have multiplied by a parameter  $\beta$  the term  $\kappa k^2 \mathcal{H}_0(k) h(-k)$  in Eq. (14) that couples the height and composition fluctuations. We find that the

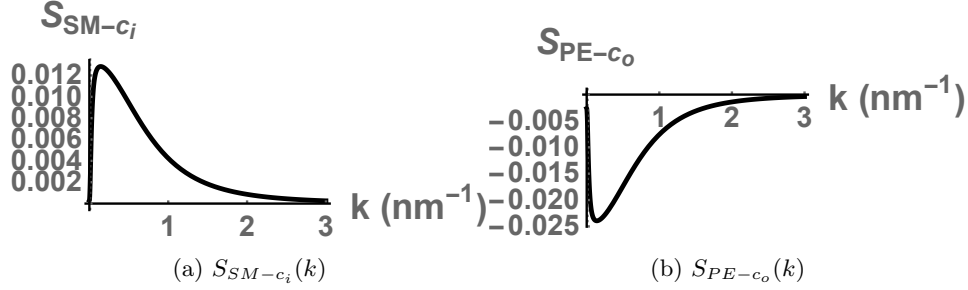


Figure 5: Two structure functions characterizing the correlation between compositions in the two leaflets.

|            |      |            |      |
|------------|------|------------|------|
| $y_{SM_o}$ | 0.18 | $x_{SM_o}$ | 0.08 |
| $y_{SM_d}$ | 0.18 | $x_{SM_d}$ | 0.08 |
| $y_{PC}$   | 0.32 | $x_{PC}$   | 0.16 |
| $y_{c_o}$  | 0.32 | $x_{c_o}$  | 0.16 |
| $y_{PS}$   | 0.18 | $x_{PS}$   | 0.09 |
| $y_{PE}$   | 0.35 | $x_{PE}$   | 0.18 |
| $y_{c_i}$  | 0.47 | $x_{c_i}$  | 0.25 |

Table 1: Lipid composition of the two leaflets is shown on the left as mol fraction in the leaflet, and on the right as mol fraction in the bilayer.

appearance of the microemulsion in the inner leaflet is quite robust. The strength of the coupling as measured by  $\beta$  would have to be reduced by more than two orders of magnitude for the inner leaflet to behave like an ordinary fluid as indicated by a peak at zero wave number in  $S_{PE-PE}(k)$ . Thus there is a very large range of values of the coupling strength over which the inner leaflet displays the properties of a microemulsion. On the other hand, we note that with a value of spontaneous curvature appropriate to PE the microemulsion is near its limit of stability. With an increase of  $\beta$  from its value of unity by about 1.7%, the correlation functions in both leaflets, shown in Fig. 6, clearly display exponentially damped oscillatory behavior because the correlation lengths have increased to 41.5 and 55 nm, larger than the wavelength of about 33 nm. An increase in the coupling strength by 2% brings about a transition to a modulated phase.

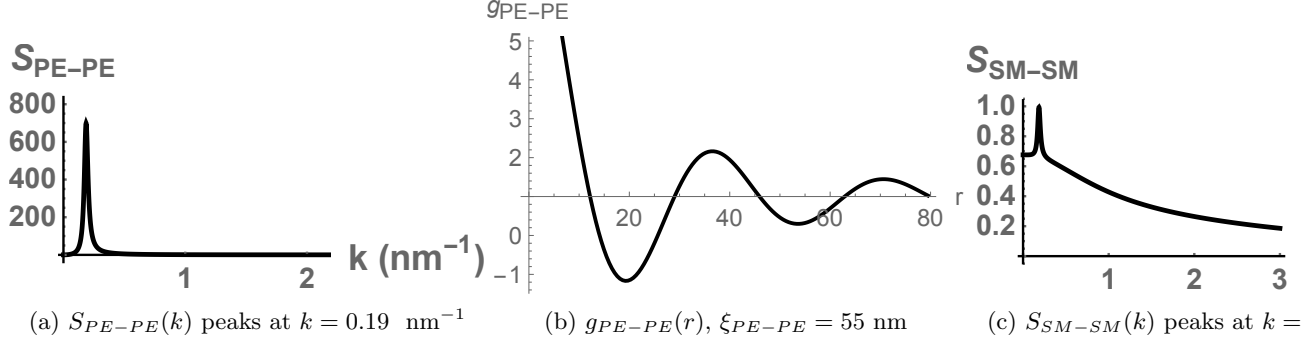


Figure 6: Exponentially damped oscillations in the correlation functions when  $\beta = 1.0165$

## 4 Conclusions

We have employed a model of an asymmetric plasma membrane with SM, PC, and cholesterol in the outer leaflet and PE, PS, and cholesterol in the inner leaflet. The membrane curvature is coupled to the concentration of PE in the inner leaflet via a cholesterol-dependent spontaneous curvature, one which reproduces the distribution of cholesterol between leaflets observed in several experiments. We find that the model predicts that the inner leaflet is almost certainly a microemulsion, but most probably a weak one with the correlation length, of order of a few nanometers or less, being much smaller than the wavelength of the spatial variations, of order 37 nm. Consequently little of the latter are seen. Whether this microemulsion propagates to the outer leaflet depends upon the strength of the coupling between leaflets.

The results of this model for the origin of “rafts” differ significantly from those of others. In particular the model states that such inhomogeneities, identified as arising from a microemulsion, originate in the inner leaflet. Furthermore because the microemulsion is weak, the model predicts that such inhomogeneities would not be present in a membrane consisting solely of lipids. However the response of the inner leaflet to external perturbations, due to non-lipid components, proteins perhaps, is largest at a distance of the order of 37 nm from the site of the perturbation. The origin of this length is clear in the model, and can be traced to the physical properties of the membrane itself via its bending rigidity and surface tension. The propagation of this response to the outer leaflet is enhanced by coupling between the leaflets.

The strength of the microemulsion, that is the degree to which spatial variations would be evident, depends in large part on the local spontaneous curvature of the membrane, which points to the importance of membrane composition. Indeed we believe that the mechanism explored here provides a plausible explanation for the modulated phases observed in the yeast plasma membrane (4) and other systems, both *in vitro*. (12–14) and *in vivo* (35). Given the close connection between modulated phases and microemulsions, it follows that these systems are very likely to display the latter as well.

## 5 Author Contributions

HG designed and performed research, and analyzed data. MS designed research, and wrote the paper.

## 6 Acknowledgments

We are grateful to Sarah Keller and Lutz Maibaum and their groups for stimulating interactions. This work was supported in part by the National Science Foundation under grant No. DMR-1203282.

## References

1. Lingwood, D., and K. Simons. 2010. Lipid rafts as a membrane-organizing principle. *Science* 327:46–50.
2. Schroeder, R., E. London, and D. Brown. 1994. Interactions between saturated acyl chains confer detergent resistance on lipids and glycosphosphatidylinositol (gpi)-anchored proteins: Gpi-anchored proteins in liposomes and cells show similar behavior. *PNAS* 91:12130–12134.
3. Veatch, S. L., and S. L. Keller. 2005. Seeing spots: Complex phase behavior in simple membranes. *Biochim. Biophys. Acta* 1746:172–185.
4. Toulmay, A., and W. Prinz. 2013. Direct imaging reveals stable micrometer-scale lipid domains that segregate proteins in live cells. *J. Cell. Biol.* 202:35–44.
5. Wang, T. Y., R. Leventis, and J. R. Silvius. 2000. Fluorescence-based evaluation of the partitioning of lipids and lipidated peptides into liquid-ordered microdomains: A model for molecular partitioning into 'lipid rafts'. *Biophys. J.* 79:919–933.

6. Matcha, B., S. Papanikolaou, J. Sethna, and S. Veatch. 2011. Minimal model of plasma membrane heterogeneity requires coupling cortical actin to criticality. *Biophys. J.* 100:1668–1677.
7. Gompper, G., and M. Schick. 1994. Self-assembling amphiphilic systems. Academic Press, San Diego.
8. Brewster, R., P. Pincus, and S. A. Safran. 2009. Hybrid lipids as a biological surface-active component. *Biophys. J.* 97:1087–1094.
9. Palmieri, B., and S. Safran. 2013. Hybrid lipids increase the probability of fluctuating nanodomains in mixed membranes. *Langmuir* 29:5246–5261.
10. Heberle, F., M. Doctorova, S. Goh, R. S. and J. Katsaras, and G. W. Feigenson. 2013. Hybrid and nonhybrid lipids exert common effects on membrane raft size and morphology. *JACS* 135:14932–14935.
11. Schick, M. 2012. Membrane heterogeneity: Manifestation of a curvature-induced microemulsion. *Phys. Rev. E.* 85:031902–1–031902–4.
12. Konyakhina, T., S. Goh, J. Amazon, F. Heberle, J. Wu, and G. Feigenson. 2011. Control of a nanscopic-to-macroscopic transition:Modulated phases in four-component dspc/dopc/popc.chol giant unilamellar vesicles. *Biophys. J.* 101:L08–L10.
13. Goh, S. L., J. Amazon, and G. Feigenson. 2013. Toward a better raft model: Modulated phases in the four-component bilayer, dspc/dopc/popc/chol. *Biophys. J.* 104:853–862.
14. Stanich, C. A., A. R. Honerkamp-Smith, G. G. Putzel, C. S. Warth, A. K. Lamprecht, P. Mandal, E. Mann, T.-A. D. Hua, and S. L. Keller. 2013. Coarsening dynamics of domains in lipid membranes. *Biophys. J.* 106:444–454.
15. Amazon, J., S. L. Goh, and G. Feigenson. 2013. Competition between line tension and curvature stabilizes modulated phase patterns on the surface of giant unilamellar vesicles: A simulation study. *Phys. Rev. E* 87:022708–1–022708–10.
16. Leibler, S., and D. Andelman. 1987. Ordered and curved meso-structures in membranes and amphiphilic films. *J. Physique* 48:2013–2018.

17. Giang, H., and M. Schick. 2014. How cholesterol could be drawn to the cytoplasmic leaf of the plasma membrane by phosphatidylethanolamine. *Biophys. J.* 107:2337–2344.
18. Brasaemle, D., A. Robertson, and A. Attie. 1988. Transbilayer movement of cholesterol in the human erythrocyte membrane. *J. Lipid Res.* 29:481–489.
19. Schroeder, F., G. Nemezc, W. G. Wood, C. Joiner, G. Morrot, M. Ayraud-Jarrier, and P. Devaux. 1991. Transmembrane distribution of sterol in the human erythrocyte. *Biochimica Et Biophysica Acta* 1066:183–192.
20. Wood, W., F. Schroeder, L. Hoky, A. Rao, and G. Nemezc. 1990. Asymmetric distribution of a fluorescent sterol in synaptic plasma membrane: effects of chronic ethanol consumption. *Biochim. Biophys. Acta* 1025:243–246.
21. Igbavboa, U., N. Avdulov, F. Schroeder, and W. Wood. 1996. Increasing age alters transbilayer fluidity and cholesterol asymmetry in synaptic plasma membranes of mice. *J Neurochem* 66.
22. Shlomovitz, R., and M. Schick. 2013. Model of a raft in both leaves of an asymmetric lipid bilayer. *Biophys. J.* 105:1406–1413.
23. Lange, Y., J. Dolde, and T. Steck. 1981. The rate of transmembrane movement of cholesterol in the human erythrocyte. *J. Biol. Chem.* 256:5321–5323.
24. Muller, P., and A. Hermann. 2002. Rapid transbilayer movement of spin-labeled steroids in human erythrocytes and in liposomes. *Biophys. J.* 82:1418–1428.
25. Putzel, G., and M. Schick. 2011. Insights on raft behavior from minimal phenomenological models. *J. Phys.:Condens. Matter* 23:284101:1–284101:–5.
26. Almeida, P. 2011. A simple thermodynamic model of the liquid-ordered state and the interactions between phospholipids and cholesterol. *Biophys. J.* 100:420–429.
27. Veatch, S. L., K. Gawrisch, and S. L. Keller. 2006. Closed-loop miscibility gap and quantitative tie-lines in ternary membranes containing diphytanoyl PC. *Biophys. J.* 90:4428–4436.



28. Hung, W.-C., M.-T. Lee, F.-Y. Chen, and H. Huang. 2007. The condensing effect of cholesterol in lipid bilayers. *Biophys. J.* 92:3960–3967.
29. Phillips, M. 1971. The physical state of phospholipids and cholesterol in monolayers, bilayers, and membranes. *Prog. Surf. Membrane Sci.* 5:139–222.
30. May, S. 2009. Trans-monolayer coupling of fluid domains in lipid bilayers. *Soft Matter* 5:3148–3156.
31. Blosser, M., A. Honerkamp-Smith, T. Han, M. Hataaja, and S. Keller. 2015. Transbilayer colocalization explained via measurement of strong coupling parameters. *Biophys. J.* 109:2317–2327.
32. Zachowski, A. 1993. Phospholipids in animal eukaryotic membranes: transverse asymmetry and movement. *Biochemical J.* 294:1–14.
33. Kawakatsu, T., D. Andelman, K. Kawasaki, and T. Taniguchi. 1993. Phase transitions and shapes of two component membranes and vesicles i: strong segregation limit. *J. Phys. II France* 3:971–997.
34. Taniguchi, T., K. Kawasaki, D. Andelman, and T. Kawakatsu. 1994. Phase transitions and shapes of two component membranes and vesicles ii: weak segregation limit. *J. Phys. II France* 4:1333–1362.
35. Lavrentovitch, M., E. Horsley, A. Radja, A. M. Sweeney, and R. D. Kamien. 2016. First-order patterning transitions on a sphere as a route to cell morphology. *PNAS* 113:5189–5194.
36. Evans, E. 1983. Bending elastic modulus of red blood cell membrane derived from buckling instability in micropipet aspiration tests. *Biophys. J.* 43:27–30.
37. Dai, J., and M. P. Sheetz. 1999. Membrane teher formation from blebbing cells. *Biophys. J.* 77:3363–3370.
38. Almeida, P. 2009. Thermodynamics of lipid interactions in complex bilayers. *Biochim. Biophys. Acta* 1788:72–85.
39. Putzel, G., M. Uline, I. Szleifer, and M. Schick. 2011. Interleaflet coupling and domain registry in phase-separated lipid bilayers. *Biophys. J.* 100:996–1004.
40. van Meer, G. 2011. Dynamic transbilayer lipid asymmetry. *Cold Spring Harb. Perspect. Biol.* 3:1–11.

- 41. Hirose, Y., S. Komura, and D. A. Andelman. 2009. Coupled modulated bilayers: A phenomenological model. *ChemPhysChem* 10:2839–2846.
- 42. Hirose, Y., S. Komura, and D. Andelman. 2012. Concentration fluctuations and phase transitions in coupled modulated bilayers. *Phys. Rev. E* 86:021916–1–13.
- 43. Lange, Y., and J. M. Slayton. 1982. Interaction of cholesterol and lysophosphatidylcholine in determining red cell shape. *J. Lipid Res.* 23:1121–1127.
- 44. Mondal, M., B. Mesmin, S. Mukherjee, and F. Maxfield. 2009. Sterols are mainly in the cytoplasmic leaflet of the plasma membrane and the endocytic recycling compartment of CHO cells. *Mol. Biol. Cell* 20:581–588.